Microstructure and hardness evolution of laser metal deposited AA5087 wall-structures

Frönd, Martin; Ventzke, Volker; Riekehr, Stefan; Kashaev, Nikolai; Klusemann, Benjamin; Enz, Josephin

Published in:
Procedia CIRP

DOI:
10.1016/j.procir.2018.08.062

Publication date:
2018

Document Version
Publisher's PDF, also known as Version of record

Available online at www.sciencedirect.com

ScienceDirect

Procedia CIRP 74 (2018) 131–135

www.elsevier.com/locate/procedia

10th CIRP Conference on Photonic Technologies [LANE 2018]

Microstructure and hardness evolution of laser metal deposited AA5087 wall-structures

Martin Froend[a,*], Volker Ventzke[a], Stefan Riekehr[a], Nikolai Kashaev[a], Benjamin Klusemann[a,b], Josephin Enz[a]

[a]*Helmholtz-Zentrum Geesthacht, Institute of Materials Research, Materials Mechanics, Joining and Assessment, Geesthacht 21502, Germany*
[b]*Leuphana University of Lüneburg, Institute of product and process innovation, Lüneburg 21337, Germany*

* Corresponding author. Tel.: +49-4152 87-2558. *E-mail address:* martin.froend@hzg.de

Abstract

Wire-based laser metal deposition enables to manufacture structures with very high deposition rates in comparison to powder-based laser additive manufacturing. However, this advantage is generally accompanied with a high energy input. Thus, an accumulation of heat within the structure can result. In addition, the heat conduction conditions can also change with increasing structure height, leading to inhomogeneous microstructural formation along the part. The present study deals with the evolution of the microstructure and hardness in laser metal deposited AA5087 wall structures. In this regard, two samples processed at adapted parameters for different deposition rates are investigated.

Keywords: laser additive manufacturing; aluminum alloy; laser metal deposition; microstructure; microhardness

1. Introduction

Recent research on additive manufacturing (AM) of metal components primarily focuses on the fabrication of complex aluminum structures using powder-based approaches such as selective laser melting (SLM) [1–3]. In SLM, it is possible to produce near net shape components with fine microstructure, resulting in high mechanical performance of the parts [3]. However, possible deposition rates of this process are still limited to several gram per minute, which limits its application to high efficient large part production [4]. In contrast to powder-based approaches, also wire-based techniques were developed and investigated in recent years, which enable a significant increase of the deposition rates up to several kilogram per hour [2,4–6]. However, processing increased deposition rates, accompanied with necessary power input adaptions, strongly affects the solidification process of the material and can reduce the resulting cooling rate, which again might lead to coarser microstructures and poor mechanical properties of the processed components, respectively. Laser sources are commonly used already in industry as energy input for fusion joining techniques, such as laser beam welding (LBW). Furthermore, since LBW is partly accompanied with filler wire injection techniques, already established machines can be easily converted to conduct wire-based laser metal deposition (LMD).

This raises the question about the effect of processing high deposition rates and high energy input in wire-based LMD of aluminum on the microstructure and resulting properties of the processed parts. For this purpose, the microstructural development with respect to different process parameters, i.e. deposition rates, using wire-based LMD for an Al-Mg alloy is investigated. Furthermore, microhardness tests of the samples are conducted and the results are discussed in relation to the microstructural observations.

2. Experimental procedure

In this study, the aluminum alloy AlMg4.5MnZr (EN AW-5087) was used for deposition on a rolled AlMg3 (EN AW-

10.1016/j.procir.2018.08.062

5457) substrate sheet in annealed and recrystallized condition. The deposition was conducted using an 8 kW continuous wave ytterbium fiber laser YLS-8000-S2-Y12 (IPG Photonics Corporation) with a wavelength of 1070 nm, which was integrated in an optical head YW52 Precitec. This configuration was handled by a CNC-supported XYZ-machining center (IXION Corporation PLC).

During the unidirectional deposition the substrate was clamped on a moving platform, and a local argon shielding was supplied to protect the molten material from undesired reaction with atmospheric elements. Additionally, a waiting time of 60 s between the depositions of two layers was applied. Table 1 summarizes the two sets of process parameters used in this study.

Table 1. Sets of process parameters used in the LMD process study.

Parameters	Set 1	Set 2	Unit
Laser power	4500	4000	W
Spot diameter	1.6	1.6	mm
Deposition rate	32	21	g/min
Deposition velocity	1	1	m/min
Energy Density	8.6	11.5	kJ/g
Line Energy	0.27	0.24	kJ/mm
Shielding gas flow rate	10	10	l/min
Number of layers	22	31	-
Height of individual layers	2.3	1.6	mm

It is well-known, that the heat transfer conditions change with increasing height of the deposited structures, also affecting the microstructural evolution in AM of aluminum parts [4]. For reasons of comparability, two LMD structures with representative heights of 50 mm and lengths of 200 mm were deposited using two different deposition rates, requiring also different laser powers (Table 1). By this, two structures having the same dimension, but consisting of a different number of layers were generated. The deposition process of a multi-layer wall structure as well as the produced specimens are shown in Fig. 1.

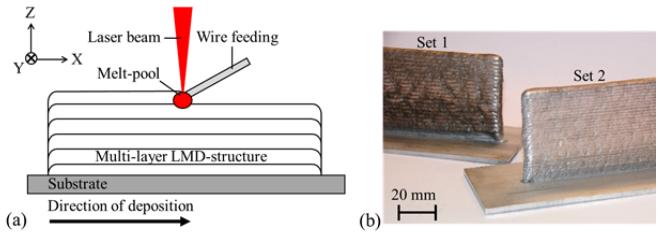

Fig. 1. (a) LMD-process setup of the unidirectional deposition process and (b) processed LMD wall structures with a height of 50 and a length of 200 mm.

3. Characterization methodology

For microstructural investigation as well as microhardness testing, three metallographic cross and longitudinal sections at different positions along the multi-layer wall structures were extracted. The selected sample positions are shown in Fig. 2. The samples were mounted, grounded and polished using an oxide polishing suspension compound (OPS). Microstructural observations were performed using an inverted optical microscope (OM) (Leica DMI 5000M) with polarized light. Since Al-Mg alloys are very corrosion-resistant and common aluminum etching agents are not sufficient to visualize the microstructure, an electrolytic etching using a 2.5%-acidiferous tetrafluoroboric acid causticise (35%) was utilized. This technique, also known as Barker method, was performed at 30 V and an exposure time of 90 s. Therefore, the microstructure images of the longitudinal sections show colored grains, which is reasoned by the use of OM under polarized light after etching the specimens. Color differences between single grains or between two images are not connected to grain size or orientation differences. The average grain size is calculated by an area analysis according to ASTM standard E 112. Microhardness testing was carried out along the cross sections by an automated Vickers hardness testing machine. For this purpose, a load of 0.2 kg and an indentation time of 15 s at an interspacing of 1 mm between the measuring locations were chosen.

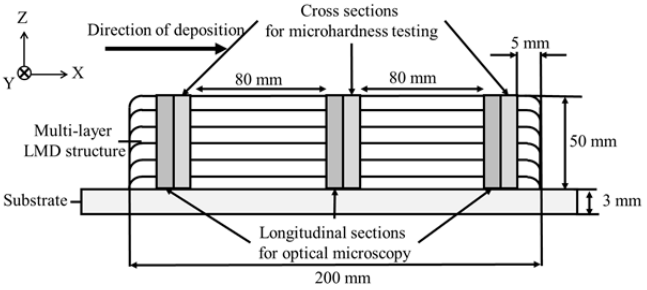

Fig. 2. Wall geometry and positions of extracted cross and length sections.

4. Results and discussion

4.1. Microstructure

Wire-based AM is a melting solidification process such as casting. Therefore, it also shows typical microstructural features such as a preferential grain growth orientation during solidification [7]. Figs. 3 (a) and (b), taken at a height of 25 mm and 100 mm in deposition direction of the samples, show one LMD layer as well as the upper and lower adjacent interlayer regions. The micrographs indicate a preferred grain growth in building direction for both parameter sets. Furthermore, the microstructures exhibit inner regions consisting of finer grains and local interlayer porosity.

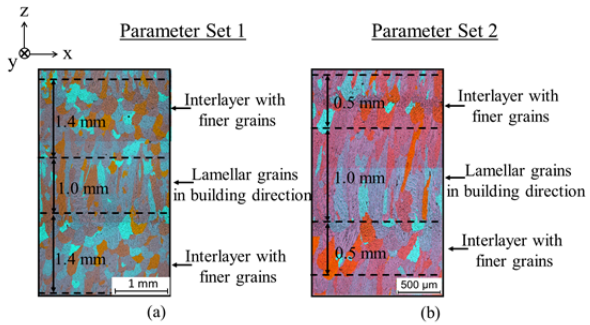

Fig. 3. OM polarized micrographs of parameter Set 1 (a) and 2 (b) showing inhomogeneous microstructure and different layer as well as interlayer thicknesses.

Zhang et.al (2018) [4] found similar microstructural features in wire and arc AM of Al-Mg alloys. By comparison of the resulting microstructures, generated by the application of parameter Set 1 and Set 2, it is noted that the sample processed at an increased deposition rate, shows an increased layer height and increased formation of larger fine-grained zones. Furthermore, an increase of a factor of approximately three, in the current case from 0.5 mm to 1.4 mm for the height of intermediated fine-grained zones, is measured. These measurements were conducted using OM micrographs, in which clear transitions between equiaxed and coarse grain orientation and morphology are visible as shown in Figs. 3 to 5.

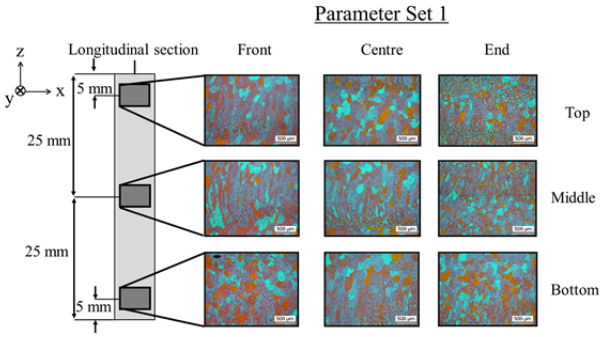

Fig. 4. OM polarized micrographs resulting microstructure for parameter Set 1.

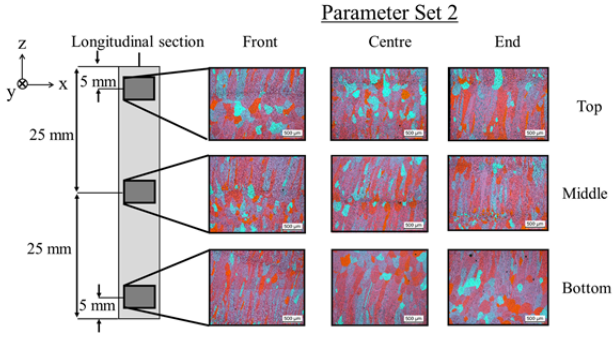

Fig. 5. OM polarized micrographs of the resulting microstructure for parameter Set 2.

The areas with columnar grains along the building direction show a height of around 1.0 mm for both parameter sets. Therefore, it is assumed that processing different deposition rate has no influence on the grain growth direction during solidification, but appears to affect the size of interlayer regions with finer grains in the current case. Due to a reduced number of layers in case of parameter Set 1, a reduced number of interlayers along the height of the sample occurred. By this, also the amount of interlayer porosity is reduced. The reason of occurring interlayer porosity is assumed to result from a developed oxide layer on the freshly deposited structure after the deposition. Since the deposited material is still very hot but the local argon shielding is not present any more after the deposition, the hot solidified material partly picks up oxides from the atmosphere from which porosity can result. Figs. 4 and 5 show the microstructures of LMD structures generated by application of the parameter Set 1 and Set 2 using longitudinal samples at different positions to examine the average grain size.

From these observations, it is assumed that the local as well as the global mechanical properties between the processed structures may vary. Both parameter sets are presumed to show slightly higher tensile strengths for loadings along the height of the structure, which is the main orientation direction of the columnar grains. The morphological grain alignment along the different positions does not show significant variations, i.e. the long axis are oriented almost parallel to height direction. However, the comparison between the specific microstructure positions yield different grain sizes along the height and the length of the structure.

The results of microscopic estimation of average grain sizes according to ASTM standard E 112 is shown in Fig. 6. It can be seen that the average grain size shows the same trend along the height of the structure for both parameter sets. The average grain size at the indicated positions at the bottom and the top of the structures is almost identical. A maximum of the grain size appears in the center region of the structure. These variations of grain sizes may be the result of locally different cooling conditions during the LMD process and solidification.

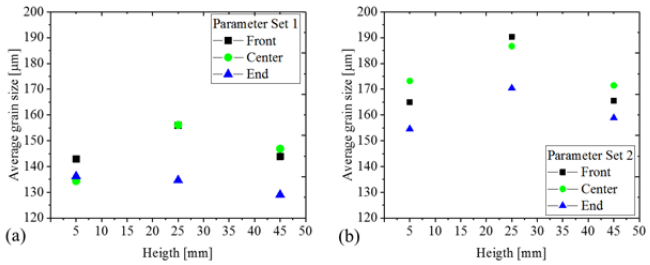

Fig. 6. Average grain sizes for parameter Set 1 (a) and Set 2 (b).

By this, it is presumed, that the cooling conditions and temperature gradients along the height of the structure vary. As already discussed in Froend et.al (2018) [7], the heat

proceeds rapidly in the substrate during the deposition of the first layers, which results in a high cooling rate, high temperature gradients and finer grains respectively. Subsequently, after the deposition of several layers and, therefore, increasing distance to the substrate, the heat conduction into the substrate is reduced. By this, the heat conduction during and after the deposition of additional layers is restricted and heat accumulates in the structure [7]. This is expressed by a decreased cooling rate and temperature gradients and the development of larger grains respectively. After the deposition process is completed and no further heat input is provided into the structure, cooling at the topside of the structure increases marginally compared to at the center. The heat accumulation in the structure is still present but decreases, since the heat is transferred by conduction and convection. Therefore, the average grain size at the topside of the structure is lower than in the center.

From Fig. 6, it is also observed that the microstructure towards the end of the structure consists of marginally smaller grains for both parameter sets. Whereas the laser source continues to heat up the structure during and after the deposition at the front and center of the structure, this is no longer the case at the end of the deposition path. After the deposition process is finished, the laser is switched off and the end region of the structure cools down more rapidly compared to the front and center region, yielding in finer grains.

Regarding the evolution of the average grain size resulting from both parameter sets, similar tendencies are observed. However, comparing the average grain sizes itself, it is shown that processing higher deposition rates has a pronounced influence in the current case. The average grain size resulting from parameter Set 1 is determined between 129 and 156 µm, whereas the grain size for parameter Set 2 is calculated to be between 155 and 190 µm. It is assumed that LMD using an increased deposition rate, which also requires an adaption of the heat input to achieve a sufficient melt pool to fully melt the material, results in a minor increase of the cooling rate. The higher heat input leads also to a temperature increase compared to processes with lower deposition rates. Therefore, the occurring temperature gradient also increases leading again to higher cooling rates during and after solidification, explaining the slightly smaller grain sizes for parameter Set 1.

4.2. Microhardness

The microhardness along the structure generated by parameter Set 1, see Fig. 7 (a), shows an average hardness of $77.3 \pm 12\,HV0.2$. Parameter Set 2 leads to an average microhardness of $74.9 \pm 4.1\ HV0.2$. The corresponding hardness profile is plotted in Fig. 7 (b). It has to be added that the hardness testing at two locations along the cross section taken from the center of the structure, namely the first 8 mm from the bottom as well as 8 mm in the center regions, were invalid due to located porosity and were omitted in order not to falsify the results. However, the microhardness in these sections is assumed to be in the range of the average microhardness value.

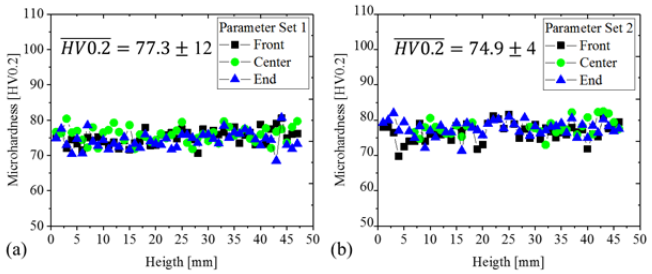

Fig. 7. Microhardness using parameter Set 1 (a) and Set 2 (b)

The comparison of the hardness profiles shows that the varied grain sizes along the structure do not have a significant effect on the microhardness. It is assumed that during microhardness testing, some indentations were located in the area of columnar grains and some in the fine-grained zones. Since the microstructure of the structure processed by parameter Set 1 shows larger areas of finer grains, this may explain the increased deviation in the microhardness measurements. However, the varying average grain diameters between these areas do not affect the microhardness evolution significantly in the current case. For future investigation explicit hardness testing using smaller indenters could be used to characterize these fine grained areas in more detail.

5. Conclusions

In this contribution, the microstructure and microhardness evolution of wire-based LMD processed wall structures using the aluminum alloy 5087 processed at two process parameter sets using adapted parameters to process different deposition rates was investigated. It was found, that varying grain sizes along the height and length of the structures are present. These variations are assumed to result from changing heat transfer conditions during the process. Larger interlayers with finer grains as well as globally finer grains along the structure for an increased deposition rate were observed. It is concluded that process parameters adapted for varied deposition rates result in different grain sizes and interlayer occurrence of finer grains along the structure height. Regarding the microhardness, no significant changes between the investigated parameter sets were observed. Although processing parameters for the increased deposition rate yields in smaller averaged grain sizes, the difference in size seems to be not significant enough to change the microhardness considerably in the current case.

Future work will address the detailed characterization of the microstructure using EBSD measurement technique as well as the mechanical testing of the samples in order to reveal the influence of the interlayer grains to the mechanical properties of the processed structure.

References

[1] Ding D, Pan Z, Cuiuri D, Li H. Wire-feed additive manufacturing of metal components: technologies, developments and future interests. Int J Adv Manuf Technol 2015;81:465–81. doi:10.1007/s00170-015-7077-3.

[2] Schmidt M, Merklein M, Bourell D, Dimitrov D, Hausotte T, Wegener K, et al. Laser based additive manufacturing in industry and academia. CIRP Ann 2017;66:561–83. doi:10.1016/j.cirp.2017.05.011.

[3] Thijs L, Kempen K, Kruth JP, Van Humbeeck J. Fine-structured aluminium products with controllable texture by selective laser melting of pre-alloyed AlSi10Mg powder. Acta Mater 2013;61:1809–19. doi:10.1016/j.actamat.2012.11.052.

[4] Zhang C, Li Y, Gao M, Zeng X. Wire arc additive manufacturing of Al-6Mg alloy using variable polarity cold metal transfer arc as power source. Mater Sci Eng A 2018;711:415–23. doi:10.1016/j.msea.2017.11.084

[5] Gu J, Wang X, Bai J, Ding J, Williams S, Zhai Y, et al. Deformation microstructures and strengthening mechanisms for the wire+arc additively manufactured Al-Mg4.5Mn alloy with inter-layer rolling. Mater Sci Eng A 2018;712:292–301. doi:10.1016/j.msea.2017.11.113.

[6] Tran H, Tchuindjang JT, Paydas H, Mertens A, Jardin RT, Duchêne L, et al. 3D thermal finite element analysis of laser cladding processed Ti-6Al-4V part with microstructural correlations. Mater Des 2017;128:130–42. doi:10.1016/j.matdes.2017.04.092.

[7] Froend M, Ventzke V, Riekehr S, Kashaev N, Klusemann B, Enz J. Microstructure and Microhardness of Wire-based Laser Metal Deposited AA5087 using an Ytterbium Fibre Laser. Mater Charact 2018:Accepted Manuscript. doi:https://doi.org/10.1016/j.matchar.2018.05.022.